Presence of Persistent Unknown Disturbances. *AIChE J.* **1980**, *26*, 247.
Nisenfeld, A. E.; Seeman, R. C. *Distillation Columns*; ISA Monograph Series 2; Instrument Society of America: Research Triangle Park, NC, 1981.
PROCESS Reference Manual; Simulation Science Inc.: Fullerton, CA, 1981; pp 9.43-9.44.
Rademaker, O.; Rijnsdorp, J. E.; Marrleveld, A. Dynamics and Control of Continous Distillation Units; Elsevier: Amsterdam, 1975.
Riggs, J. Letter to the editor. *AIChE J.* **1990**, *36* (7), 1124-1125.
Ryskamp, C. Using Probability Axis for Plotting Composition Profiles. *Chem. Eng. Prog.* **1981**, *77*, 42-47.
Skogestad, S.; Morari, M. Understanding the Dynamic Behavior of Distillation Columns. *Ind. Eng. Chem. Res.* **1988a**, *27*, 1848-1862.
Skogestad, S.; Morari, M. LV-Control of a High-Purity Distillation Column. *Chem. Eng. Sci.* **1988b**, *43* (1), 33-48.
Strang, G. Linear Algebra and its Applications; Harcourt Brace Jovanovich: New York, 1980.
Weber, R.; Brosilow, C. B. The Use of Secondary Measurements to Improve Control. *AIChE J.* **1972**, *18*, 614-623.
Whitehead, D. B.; Parnis, M. Computer control improves ethylene plant operation. *Hydrocarbon Process.* **1987**, 105-108.

Received for review March 19, 1991
Accepted July 23, 1991

Composition Estimator in a Pilot-Plant Distillation Column Using Multiple Temperatures

Thor Mejdell and Sigurd Skogestad*
Chemical Engineering, University of Trondheim, NTH, N-7034 Trondheim, Norway

Results are given for the implementation of a static partial least-squares (PLS) regression estimator for product compositions on a high-purity pilot-plant distillation column. Temperatures on all 11 trays are used as inputs to the estimator. Several estimators were tested off line to compare their performance, and one estimator was used on line for dual composition control. It was found that the estimators perform very well when appropriate logarithmic transforms and scalings are used. Since the estimator is static, the implementation is straightforward. An estimator based only on experimental data gave excellent performance over a wide range of operating points. Estimators based on simulations did not perform quite as well, and the bias had to be adjusted when a change was made from one operating point to another. Nevertheless, since it may be difficult to obtain good experimental data in an industrial setting, this estimator is probably most useful in practice. In this paper we also discuss how to combine information from simulations (basic modeling) and experiments.

1. Introduction

Product composition analyzers for distillation columns, such as gas chromatographs, have large investment and maintenance costs, in addition to unfavorably large measurement delays. The most popular means of product control is therefore temperature control (Kister, 1990), which provides an easy, fast, and inexpensive means of composition control.

The temperature selected for control is usually located at a tray some distance away from the column ends, because the products may be extremely pure, and the temperature variations are then small compared to the noise. Furthermore, pressure variations and off-key components will interfere with the relationship between product composition and temperature and locating the measurements away from the ends is favored (Rademaker et al., 1975, p 421). However, if the measurement is located too far from the end the temperature will be strongly influenced by the composition of the feed and of the product at the other column end.

An important issue in conventional temperature control is therefore to find the best measurement location by making proper compromises between these considerations.

However, some of the interferences may be handled by using more measurements. For example, since the column pressure has about the same effect on all temperatures in the column, the pressure variation may be compensated for using temperature differences. This requires an additional temperature measurement which preferably is located at a tray where the composition is almost constant. Along the same line of thought are the proposals to use double differential temperatures. Yu and Luyben (1984) proposed use of the other differential temperature for off-key-component compensation, while Luyben (1969) and Boyd (1975) proposed using it for column-pressure-drop compensation. However, these ideas do not seem to be widely applied.

On the other hand, for the case of high-purity columns with large relative volatility between the components, the use of multiple temperatures has found some applications because the conventional temperature control is difficult. In these columns the main temperature drop will take place in a small region consisting of only a few trays. Quite small deviations from the normal operating point may lead to a control temperature outside this region. On the other hand, the location of this temperature front (region) is usually closely correlated to the compositions and may alternatively be the control objective. Bozenhart (1988) located the front by scanning multiple temperatures for the maximum temperature drop between two trays. Luyben (1971) suggested tracking the temperature front by using an average of many tray temperatures. Whitehead and Parnis (1987) used a weighted average of many differential temperatures in a C_2 splitter.

A more rigorous means of using multiple temperatures is to provide an estimator for product compositions. Many approaches have been proposed, e.g., by Brosilow and co-workers (Weber and Brosilow, 1972; Joseph and Brosilow, 1978), who used temperatures together with stream measurements and a linearized process model, and by Marquardt (1989), who used a state space observer for the location of the temperature front.

0888-5885/91/2630-2555$02.50/0

In another paper by Mejdell and Skogestad (1991a) three different estimators were compared on a rigorous basis using *linear* data for a 40-tray high-purity binary example column with a constant relative volatility of 1.5. These estimators were the dynamic Kalman–Bucy filter (Kalman and Bucy, 1961), the static Brosilow inferential estimator (Weber and Brosilow, 1972; Joseph and Brosilow, 1978), and the static principal-component-regression (PCR) estimator. It was found that for feedback control the static PCR estimator performed almost as well as the Kalman filter. The reason is that the temperatures and compositions have similar dynamic responses. The Brosilow estimator was very sensitive to model error for this ill-conditioned plant with large relative gain array (RGA) values. Mejdell and Skogestad (1991a) therefore recommended using the simple regression estimator, which is obtained simply by considering corresponding values of temperatures and composition.

Mejdell and Skogestad (1991b) further investigated the use of regression estimators in a *nonlinear* simulation study of the same column. The impact of different levels of temperature noise, pressure variations, and off-key components was also studied. The estimators were found to yield satisfactory estimates, especially when proper weighting (scaling) and logarithmic transforms were used. The use of multiple temperatures by the estimators effectively counteracted the effect of pressure variations, measurement noise, off-key components, and the nonlinearity in the column. The PLS and PCR estimators were also compared, and the first was found to be slightly better.

These results are the starting point of the present paper. We will present some of the results from an implementation of the PLS-regression estimator on a pilot-plant distillation column and discuss some issues that may be important when the estimator is implemented on industrial columns. The pilot column separates a binary mixture of ethanol and butanol and has temperature measurements on all 11 trays.

2. Experimental Equipment

2.1. The Pilot-Plant Column. The experimental distillation column (Figure 1) consists of 11 sieve trays and has a diameter of 125 mm. The space between the trays is 300 mm. A kettle type reboiler is heated by electrical elements with a total power of 15 kW. The reboiler contains 6–7 L of liquid. A water-cooled total condenser is placed right in the top of the column and is open to the atmosphere. A small accumulator tank is placed at the floor. It contains about 250 mL of distillate.

The feed and reflux flows are provided by two metering pumps with a capacity of 1 L/min. The pumps have a variable stroke length driven by a servo motor. Both flows have preheaters with temperature controllers. The distillate and bottom-product flows are adjusted to keep the reboiler and condenser levels constant (LV configuration). The bottom product will normally have the same composition as the liquid from the bottom tray (insignificant thermosyphon effect in the reboiler).

Two solenoid valves are used for sampling the liquid from the bottom and top products. They are placed below the bottom tray and after the accumulator. Because of the small accumulator size, this will imply a composition lag of, at most, 1–2 min for the dynamic test runs. The liquid samples are analyzed off line by a Chrompack 9000 gas chromatograph.

Each tray in the column is equipped with a cromel–alumel thermocouple placed in the liquid. There is also a thermocouple in the reboiler. Differential pressure cells are used for measuring the pressure drop in the tower and

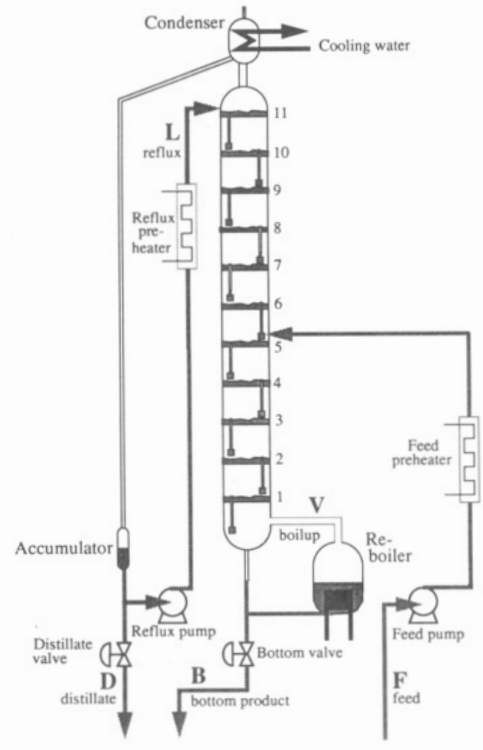

Figure 1. Pilot-plant distillation column.

liquid levels in the accumulator and reboiler.

The column may be run under a wide range of operating conditions. Typical flow rates are $F = 4.5$ and $V = 8.0$ mol/min. The vapor and liquid rates may be run from about 20 to 100% without flooding, weeping, or serious entrainments.

2.2. Data Sampling and Control. The twelve temperatures and the two level measurements are sampled every second. Every fifth second an average value is stored and control signals are sent to the four actuators. They are the two controller valves for the product flows, the power to the reboiler, and the metering pump for the reflux flow.

Liquid sampling of the distillate and the bottom products are controlled by the computer and taken precisely every second minute.

The controller loops are implemented as ordinary PID controllers with antiwindup.

2.3. Chemical Components. In the search for a suitable binary mixture, we considered the following criteria:

(1) The mixture should have a high relative volatility in order to get a high-purity distillation column. (The column has only 11 trays.)

(2) The mixture should be reasonably ideal to avoid a bias of the results from unusual VLE behavior.

(3) The mixture should be relatively convenient to handle, i.e., it should have low toxicity, relatively low flammability, have boiling temperatures around 100 °C, and be simple to analyze.

(4) The mixture should be inexpensive.

We found the mixture ethanol/1-butanol suitable for most of these requirements. It has a nearly constant relative volatility of 4.3 (Hellwig and van Winkle, 1953).

3. Data Treatment and Multivariate Regression

Multivariate calibration (regression) is a statistical approach for obtaining a linear estimator based on a "training" set of known values of inputs and outputs. For the distillation column we want to obtain the matrix $\mathbf{K}$ in

$$\hat{y} = \mathbf{K}\theta + \mathbf{k}_0 \qquad (1)$$

Here $\hat{y}$ denotes the outputs of the estimator (compositions of top product, y_D, and bottom product, x_B), and θ, the inputs (temperatures). The vector $\mathbf{k}_0$ is the bias or mean of the outputs.

A training set (calibration set) of n runs of corresponding values of θ and y are obtained and lined up in two matrices $\mathbf{Y}$ and Θ such that measurements of each run are placed in one row. Deviation variables are used; that is, all measurements are first centered around the mean in the calibration set, y_0 and θ_0. The data are in most cases also weighted (scaled). Using 2 y variables and 12 θ variables we get

$$\mathbf{Y}^{n\times 2} = \Theta^{n\times 12}\mathbf{K}^{\mathbf{T}} \tag{2}$$

where $\mathbf{K}$ has the dimension 2×12. We search for the solution

$$\mathbf{K}^{\mathbf{T}} = \Theta^{\dagger}\mathbf{Y} \tag{3}$$

where $\Theta^{\dagger}$ denotes some pseudoinverse of Θ.

Different regression methods yield different solutions for $\Theta^{\dagger}$. Using singular-value decomposition (SVD), we obtain the principal-component-regression (PCR) estimator. Here, in order to avoid collinearity and an ill-conditioned estimator, we delete the directions in Θ with small singular values (corresponding to noise). The number of remaining nonzero singular values, or equivalently the number of principal components (factors) used, will give the rank, k, of $\Theta^{\dagger}$. In our application on distillation columns, k is typically 3–5 (Mejdell and Skogestad, 1991b).

The partial least-squares (PLS) regression method used in this paper is very similar, but it also takes into account the covariance between the θ and the y variables. This may yield an estimator with fewer factors than PCR (Höskuldsson, 1988). However, Mejdell and Skogestad (1991b) found that the differences were rather small for their distillation column example. The PLS procedure is given by Martens and Næs (1989) and is also explained by Mejdell and Skogestad (1991b).

Another useful way to think about the PCR and PLS methods is in terms of latent variables: The 12 (in our case) θ variables are reduced ("averaged") to k latent variables. These latent variables are subsequently regressed with the y variables.

3.1. Use of Transformed Variables. The composition and temperature profiles are nonlinear functions of the operating variables. Logarithmic transformation of the product compositions, for example

$$Y_D = \ln (1 - y_D); \quad X_B = \ln x_B \tag{4}$$

has been proposed by several authors (e.g., Joseph et al., 1976). A more general transformation is (for binary systems)

$$X = \ln\left(\frac{x}{1-x}\right) \tag{5}$$

which also applies for trays inside the column. Here x is the tray composition (the subscript i on x to denote tray number has been omitted to simplify notation). This transformation linearizes both the dynamic *response* as well as the composition *profile* (Mejdell and Skogestad, 1991b). Temperature is often a nearly linear function of composition. Mejdell and Skogestad (1991b) therefore proposed to use the following transformation on each tray temperature θ

$$L_T = \ln\left(\frac{\theta - T_L^b}{T_H^b - \theta}\right) \tag{6}$$

Here T_L^b and T_H^b are the boiling temperatures of pure light and heavy components, respectively. We have $L_T \approx -X$. A column with pinch zones around the feed will not have a linear profile.

Instead of using boiling temperatures, one may use the transformation

$$L_\theta = \ln\left(\frac{\theta - \theta_L}{\theta_H - \theta}\right) \tag{7}$$

where θ_L and θ_H is some *reference temperature* (usually measured) in the top and the bottom of the column, respectively. For binary mixtures, one may use the temperature at the column end, which is very close to the boiling temperature and which does not change very much with operating condition. To avoid large effects of noise on the temperatures closest to the reference temperatures, one should also specify a lower permitted limit on the difference temperatures in eqs 6 and 7.

Using reference temperatures also provides pressure compensation for the temperature measurement.

3.2. Scaling of Variables, Weight Functions. In all cases the data were centered around the mean. In most cases the temperatures were weighted. Weight 1 is given by

$$W_{1i} = 1/s_{ci} \tag{8}$$

This is the inverse of the standard deviation of temperature i in the calibration set and ensures, for example, that variable scaling does not bias the results. Weight 3 (the numbering follows Mejdell and Skogestad, 1991b) is defined as

$$W_{3i} = \frac{1}{s_{ci}}\frac{s_{ci} - s_{ei}}{s_{ci}} \tag{9}$$

Here s_{ei} is the residual standard deviation ("mismatch") between the model predictions and the observations. s_{ei} takes into account both noise and mismatch due to nonlinearity. In our example s_{ei} is the residual after three PLS factors based on a preliminary calibration without weighting. Weight W_3 is equal to W_1 when the model is perfect (no noise), but gives zero weight to measurements when all the variation is unexplained ($s_{ci} = s_{ei}$).

4. Experiments and Simulations

4.1. Experimental Steady-State Runs. In order to obtain a calibration set, 19 different steady-state runs were performed on the experimental column. The runs were first checked for consistency and outliers (using the UNSCRAMBLER software package). Two runs were deleted from the calibration set during this check. The remaining 17 runs are listed in Table I. To ensure that the different directions should be present in the calibration set, a fractional design was adapted. The obtained values of y_D and x_B show some minor deviations from the original design. Nevertheless, the runs do have a good spread. We stress that it may be very difficult and time consuming to obtain such good data on an industrial column.

The column profile was "stabilized" by controlling the temperatures on tray 3 with the reboiler heat input and on tray 9 with the reflux pump. When the column temperatures had been constant for at least 10 min, samples of the feed and the product streams were taken. In addition, the average and the standard deviation of all temperatures, pressures, and output signals during the last 5–10 min were calculated and stored.

4.2. PLS Estimators Based on Experimental Runs. Different transforms of the experimental data give three different PLS estimators, denoted E1, E2, and E3.

Estimator E1 uses no logarithmic transformation. The temperatures were weighted with weight function W_1. The

Table I. The 17 Experimental Steady-State Runs Used for Obtaining Estimators E1–E3[a]

run no.	F/(mol/min)	L/F	z_F %	y_D %	x_B %
1	4.12	2.055	45.02	99.20	0.37
2	4.14	1.782	45.71	99.64	0.64
3	3.65	0.878	34.63	99.67	0.88
4	3.64	1.558	34.32	96.82	0.16
5	4.57	3.317	34.58	98.81	0.16
6	4.57	3.187	34.53	99.15	0.27
7	3.65	0.787	34.53	99.50	0.95
8	3.63	0.734	54.61	96.81	1.10
9	4.56	2.105	54.61	95.54	0.11
10	4.55	0.636	54.36	99.10	2.66
11	3.64	4.148	55.28	99.13	0.22
12	4.58	0.946	55.60	99.27	2.18
13	4.22	1.914	50.79	99.01	0.36
14	4.48	2.204	50.70	97.71	0.22
15	3.36	1.393	44.03	99.50	0.31
16	3.35	3.464	42.95	99.14	0.25
17	3.39	2.020	45.70	99.41	0.33

[a] Typical results are shown in Table III.

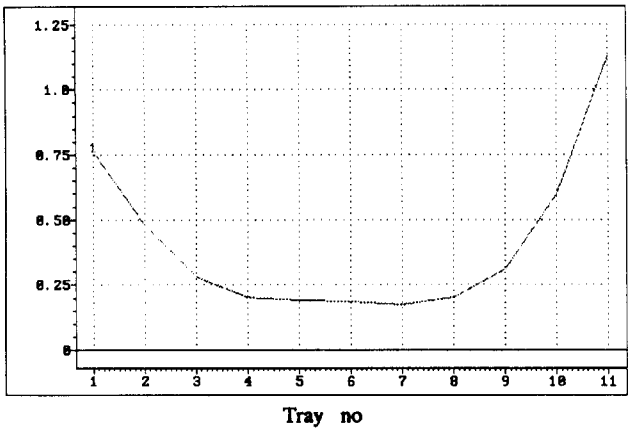

Figure 2. Weight W_1 for estimator E1.

weight is shown in Figure 2. The optimal number of factors was found to be four.

Estimator E2 also contains four factors but was obtained using the logarithmic transforms of the compositions (Y_D and X_B) in eq 4. No weighting was performed.

Estimator E3 uses, in addition to the logarithmic transform of the compositions, also the transform L_θ (eq 7) on the temperatures. The temperature in the reboiler, θ_0, was not found suitable as a reference temperature, so the temperature on tray 1 was used instead. The number of inputs to the estimator then became 9 for this estimator (compared to all 12 temperatures for E1 and E2). The data were weighted with the weight function W_3. The optimal number of factors was found to be three. W_3 and s_e is plotted in Figure 3.

4.3. PLS Estimators Based on Simulation Runs. For simulating the experimental column, a steady-state simulation program assuming constant relative volatility and constant molal flows was employed. To obtain the estimators, we used 32 different simulation runs, as listed in Table II. From experimental runs a correlation between the column pressure drop ΔP (atm) and the boilup V (mol/min) was found and included in the simulation program:

$$\Delta P = 0.0166 - 0.00140V + 0.0003482V^2 \quad (10)$$

From literature data (Helwig and van Winkle, 1953; Gay, 1927), the relative volatility of ethanol/butanol was estimated to be 4.3. To obtain a model of the column one generally adjusts the number of theoretical trays to match the experimental data. We used a constant Murphee tray

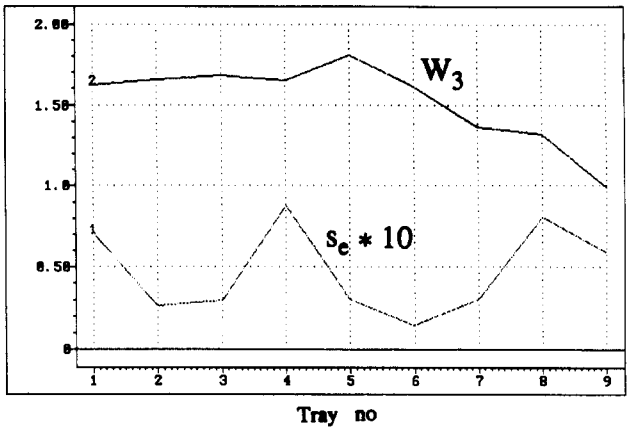

Figure 3. Residual standard deviation $s_e \times 10$ and corresponding weight W_3 used for estimator E3. Logarithmic transformed temperatures are used.

Table II. The 32 Simulated Steady-State Runs Used for Obtaining Estimators S1 and S2

F/(mol/min)	z_F	y_D	x_B	P/atm
4.5	0.5000	0.9900	0.0100	0.993
4.2	0.4875	0.9962	0.0189	1.000
4.6	0.5375	0.9913	0.0262	1.003
4.0	0.4750	0.9956	0.0087	0.991
4.3	0.4250	0.9738	0.0151	0.990
4.8	0.5625	0.9934	0.0115	0.996
4.7	0.5250	0.9700	0.0132	1.005
4.5	0.4625	0.9772	0.0300	0.998
4.1	0.4125	0.9801	0.0058	0.997
5.0	0.4375	0.9950	0.0038	1.004
4.4	0.6000	0.9849	0.0044	0.995
4.3	0.4500	0.9924	0.0173	0.992
4.9	0.5125	0.9942	0.0066	0.992
4.6	0.5750	0.9868	0.0228	1.007
4.8	0.5500	0.9827	0.0076	0.999
4.2	0.5875	0.9885	0.0050	1.010
5.0	0.4000	0.9700	0.0300	0.993
4.0	0.4000	0.9700	0.00333	0.991
4.0	0.4000	0.99667	0.0300	0.990
5.0	0.4000	0.99667	0.00333	0.998
4.0	0.6000	0.9700	0.0300	1.010
5.0	0.6000	0.9700	0.00333	0.997
5.0	0.6000	0.99667	0.0300	0.990
4.0	0.6000	0.99667	0.00333	0.999
4.25	0.4500	0.98268	0.01732	0.996
4.75	0.4500	0.98268	0.00577	1.005
4.75	0.4500	0.99423	0.01732	0.993
4.25	0.4500	0.99423	0.00577	0.992
4.75	0.5500	0.98268	0.01732	1.005
4.25	0.5500	0.98268	0.00577	0.993
4.25	0.5500	0.99423	0.01732	1.002
4.75	0.5500	0.99423	0.00577	0.990

efficiency η_M throughout the column. Simulations were performed (and estimators obtained) for the following two cases: *estimator S1*, using an average Murphee's tray efficiency, η_M, of 0.82; *estimator S2*, using a correlation between the Murphee efficiency and the boilup V and reflux L (mol/min)

$$\eta_M = 0.041L - 0.046V + 0.928 \quad (11)$$

During the experiments L and V varied in the range 3–15 mol/min. A typical temperature profile comparison is shown in Figure 4. The match with the experimental data is slightly better for case 2.

Both estimators S1 and S2 are based on logarithmic transforms on both compositions and temperatures and use weight function W3. The residuals s_{ei} for W_3 in eq 9 were found by first corrupting the data with 0.1 °C random noise and performing a preliminary calibration. Afterward the weight function from this calibration was used with

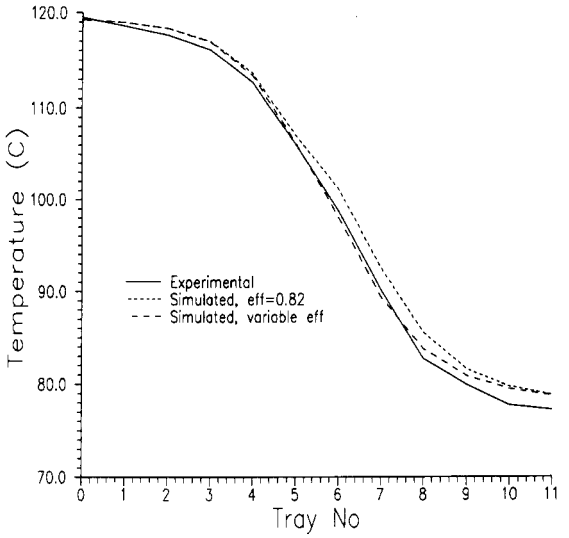

Figure 4. Comparison of temperature profiles for experimental run 16.

the original uncorrupted data in a new calibration step to obtain S1 and S2.

4.4. Dynamic Test Runs. Two test runs with large composition variations were performed for comparing the different estimators. At distinct times, usually every second minute, a liquid sample was taken and analyzed off line. Various feed and composition disturbances and set-point changes were introduced during these tests. The column was controlled using the LV configuration, i.e., the top composition was controlled by the reflux L and the bottom composition by the boilup V.

In the first test run, denoted DYN1, the column was operated by temperature control on trays 3 and 9. The column was switched between one-point control and two-point control. In one-point control large changes in reboiler power were made, while in two-point control large set-point changes were performed. The column was also subjected to disturbances in feed rate, F, and feed composition, z_F, of about 30%.

In the second test run, DYN2, the estimator S2 was used in the feedback loop, and set-point changes in the estimated values of y_D and x_B were performed. In addition a 25% increase in feed rate was introduced at time t = 29 min, a 10% decrease in feed rate, at t = 43 min; and a 30% decrease in feed composition, at time t = 53 min. The estimator S2 was corrected for bias before starting.

Controller Tunings for Test Run DYN2. Each composition control loop was first submitted to a Ziegler–Nichols tuning test, letting the other loop stay in manual. These individual Ziegler–Nichols PI parameters were then detuned by a factor f to compensate for interactions between the loops.

$$k = \frac{k^{ZN}}{f}; \quad \tau_I = f\tau_I^{ZN} \tag{12}$$

This is similar to the BLT procedure of Luyben (1986).

On the basis of the results of Skogestad and Lundström (1990) who studied PID control of a similar column, we first selected f = 2. However, additional detuning was found necessary, and f = 2.5 was used.

5. Results

5.1. Experimental Steady-State Runs. The results of all steady-state runs are given in the thesis of Mejdell (1990). In Table III the results from a typical run are shown. The standard deviations of the temperatures in the middle of the column are approximately 10 times larger than those at the ends. They are clearly related to the slope of the temperature profile, as seen from the dotted line in Figure 5. Consequently, most of the noise on the temperatures seems to be related to the liquid flow and mixing on the trays and *not* to the measurement device.

In Figure 6a the temperature profiles for runs 5–8 are displayed. The corresponding logarithmic profiles are seen in Figure 6b. The linearizing effect on the profile is clear, except for the top section of run 8 which has a pinch zone around the feed tray.

5.2. Experimental Test DYN1. The estimators were compared off line using experimental temperature data from DYN1. The estimates of the experimentally based estimators E1 and E2 are displayed in Figure 7. Estimator E1 performs well for y_D but not as well for x_B. Although it tracks the main changes, it has a tendency to overdo them and also gives negative values of x_B. On the other hand, estimator E2 yields excellent bottom-product estimates, while the top-product estimate shows some steady-state offset. Note that the use of logarithmic transformed compositions in this case guarantees that the estimates of x_B and y_D stay between 0 and 1.

Table III. Data from a Typical Steady-State Experimental Run[a]

measurement	av	std dev
temp reboiler/°C	119.1208	0.0145
temp of tray 1/°C	117.6565	0.0312
temp of tray 2/°C	115.7841	0.0498
temp of tray 3/°C	112.2051	0.1026
temp of tray 4/°C	107.0069	0.1371
temp of tray 5/°C	99.4882	0.1676
temp of tray 6/°C	92.5084	0.1531
temp of tray 7/°C	85.3724	0.0987
temp of tray 8/°C	80.5095	0.0516
temp of tray 9/°C	79.0260	0.0295
temp of tray 10/°C	77.6493	0.0203
temp of tray 11/°C	77.5407	0.0123
reboiler level/cm	7.9115	0.0551
accumulator level/cm	12.8806	0.1015
diff pressure/(cm H_2O)	16.6909	0.0476
output signals to actuators:		
reboiler duty/V	3.0499	0.0000
distillate pump/V	2.4296	0.0337
bottom valve/V	8.7820	0.1436
distillate valve/V	5.0953	0.0994

[a] Data taken during 10 min for run 3.

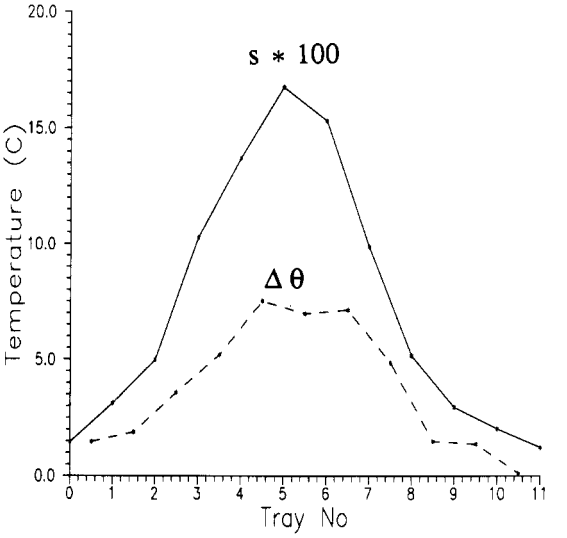

Figure 5. Comparison of standard deviation of the temperature measurements and the temperature difference $\Delta\theta$ between the trays (see Table III). Experimental steady-state run 3.

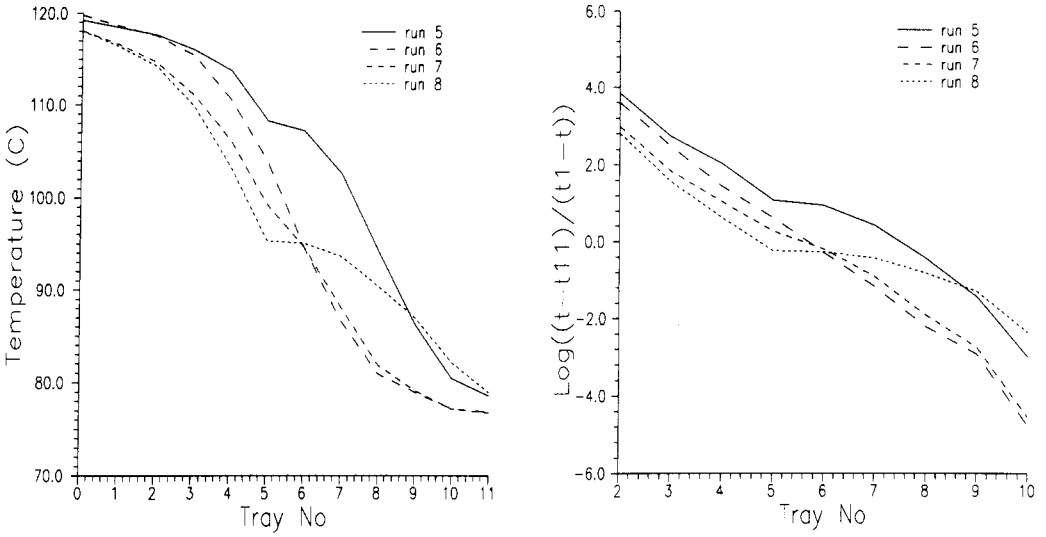

Figure 6. Temperature profiles for runs 5–8: (a) temperatures, θ; (b) logarithmic transformed temperatures, L_θ.

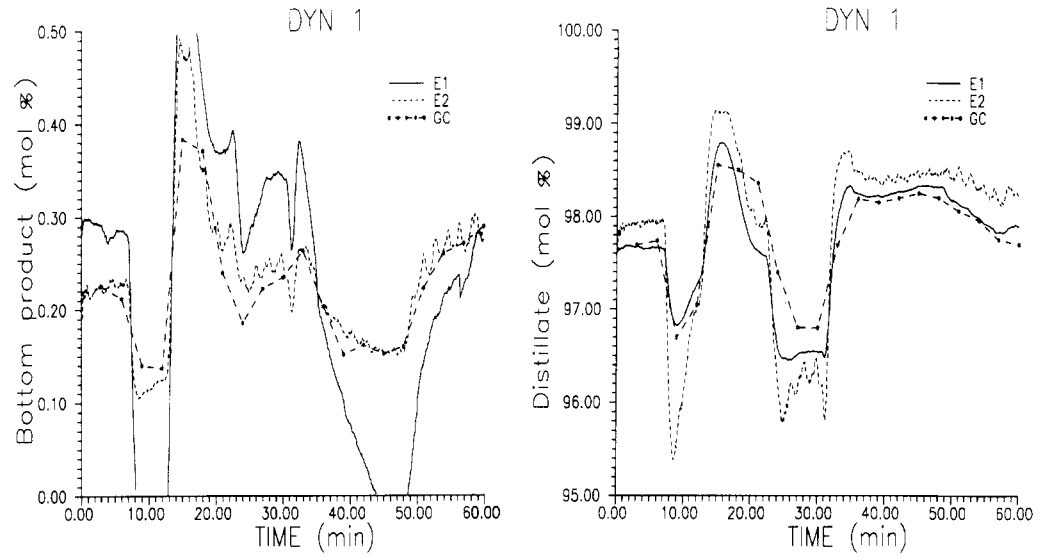

Figure 7. Performance of experiment-based estimators E1 and E2 in test DYN1.

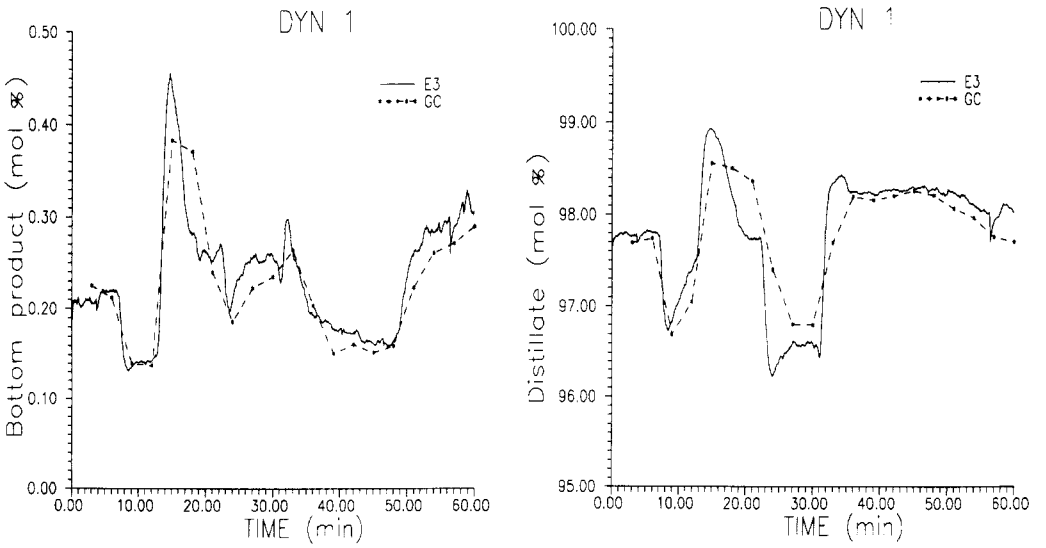

Figure 8. Performance of experiment-based estimator E3 (with logarithmic temperatures) in test DYN1.

The effect of using logarithmic transforms both for compositions and temperatures is shown in Figure 8, where estimator E3 is employed. The estimates are excellent both for top and bottom compositions. Note that the bias term $\mathbf{k}_0$ was not adjusted from its original value for any of the experimental estimators, E1, E2, and E3.

The performances of the estimators based on simulations, S1 and S3, are shown in Figure 9. The difference between S1 and S2 is minimal. In both cases the bias term $\mathbf{k}_0$ in the estimator had to be adjusted for off sets before

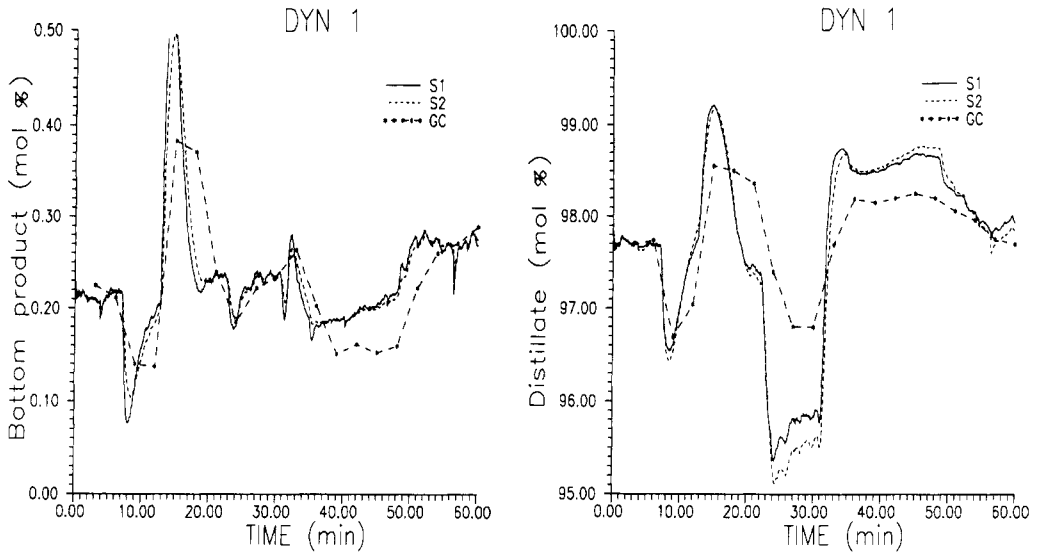

Figure 9. Performance of simulation-based estimators S1 and S2 in test DYN1.

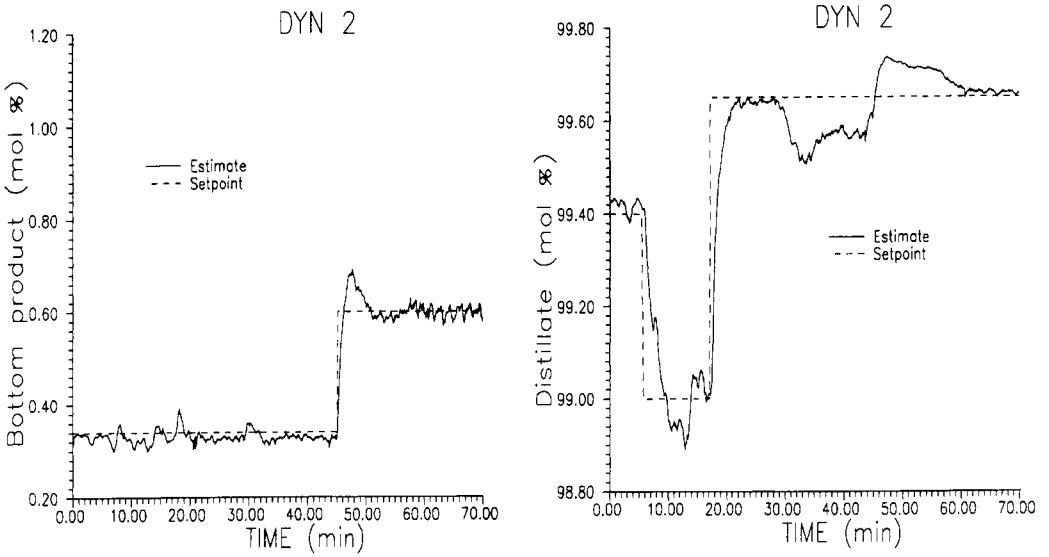

Figure 10. Control performance in test DYN2. Plot shows how well the *estimated* compositions (estimator S2) track the set point.

starting. Although the estimators based on simulations are not as good as the experimental estimator, E3, they still show reasonably good performance.

5.3. Experimental Test DYN2. In Figure 10 the set points and the *estimated* outputs are shown for the dynamic test DYN2, where estimator S2 was used on line as part of the control loop. This plot shows the control performance and not the estimator performance. The controller tracks the set points very well, and interactions between the loops do not seem to cause problems. In Figure 11 the *GC-analyzed* compositions are compared with the estimate. We see that the S2 estimates deviate substantially for the bottom composition when moving to the new operating point.

For comparison the estimates of the experimental obtained estimator E3 is also displayed in Figure 11. We note that E3 is much more sensitive to changes in the bottom product. Again, it was not subjected to any offset adjustments, whereas the bias for S2 was adjusted.

The trend of the other estimators E1, E2, and S1, was similar to those for the test DYN1.

6. Discussion

The results confirm that a static estimator is sufficient for the distillation column. The estimates are generally a little ahead in time compared to the actual compositions. This is mainly due to the lag in the accumulator and the transport delay from tray one to the solenoid valve for bottom-product sampling. This elimination of the lag is clearly an additional advantage of using temperature measurements for feedback control.

The accuracy of the estimators is also satisfactory, especially for the experimentally based estimators. Even without adjusting the bias these estimators gave very little steady-state offsets. The experimental calibration runs were obtained over an extended period of time (more than a month) and about half a year before the dynamic test DYN2. This indicates that it may not be necessary to update these estimators.

6.1. Experimental Estimators. A comparison for test DYN1 between the experimentally obtained estimators E1 and E2 (none of these use logarithmic temperatures) shows that E1 performed best for the top composition and E2 best for the bottom composition. The reason is the difference in purety for x_B and y_D in DYN1: x_B varies from 0.15 to 0.40 mol %, while $1 - y_D$ varied from 1 to 3 mol %. The logarithmic transforms of the compositions (E2) will perform best in the pure range, that is, for x_B.

The estimator with the best overall performance is E3, which seems to provide accurate estimates over a wide

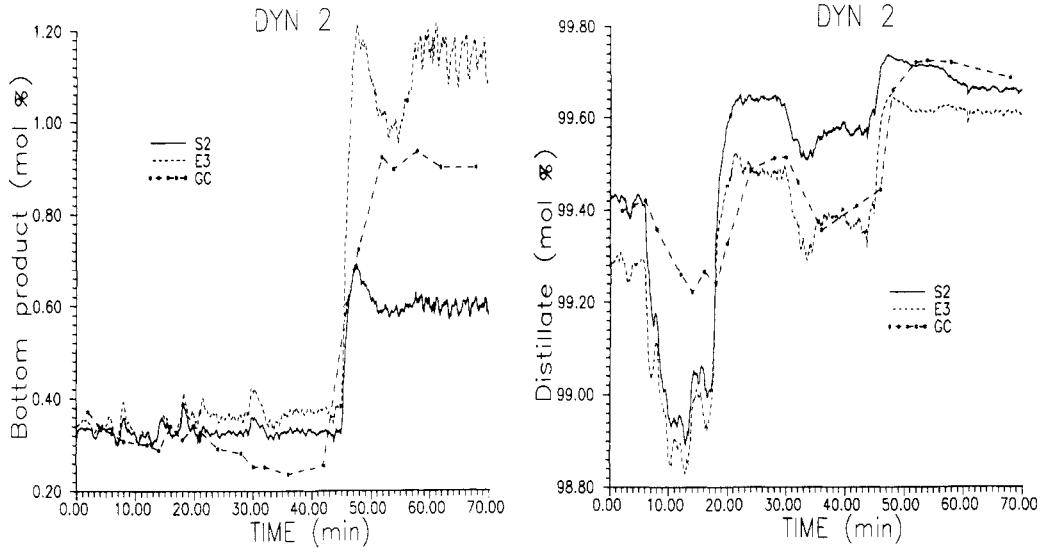

Figure 11. Performance of estimators S2 and E3 in test DYN2.

range of operations. This is primarily due to the linearizing effect of using logarithmic transformed temperatures. This confirms the results of Mejdell and Skogestad (1991b) who introduced logarithmic transformed temperatures and found them to give a substantial improvement in the steady-state accuracy.

6.2. Controller Tuning. Tuning of the control loops with the estimator on line was straightforward. The Ziegler–Nichols tuning procedure proved to work, although a substantial detuning was necessary. The estimator (and thereby also the controller) employs temperatures from both sections. One might consequently expect additional interactions between the loops. In this column, however, the interactions were not a large problem. In case it should happen to be a problem, one might consider using temperatures from the top section of the column for estimating y_D and only the bottom section for x_B. This might also be necessary if the column sections have very different dynamic responses.

6.3. Simulation Estimators. A comparison of the two simulation-based estimators S1 and S2 shows small differences. Thus, the effect of varying tray efficiency in the simulation runs thus seems to be of minor importance for this column.

The static accuracy of the simulation-based estimator S2 was not satisfactory for the bottom product in the test DYN2. This estimator must consequently be updated when a change is made from one operating point to another. Since the experimentally obtained estimator E3 performed better, it may give insight to look at the differences of the **K** matrix (eq 1) elements between estimator E3 and S2, as shown in Figure 12. We see that it is mainly the feed-tray element (tray 5) that differs. By adjusting this element in estimator S2, we found that the estimator could give excellent response for DYN2 (as well as for DYN1). This illustrates that the estimator may be quite sensitive for mismatch between the simulated and the experimental data, in particular, at trays where the **K**-matrix elements show large changes from one tray to another.

For a given estimator, one might use some test runs, such as test DYN1 and DYN2, to "adjust" a coefficient in the **K** matrix, as discussed above. A more rigorous approach would be to get a better estimator in the first place. For our column we could possibly have improved the simulation-based estimator by including (1) different tray efficiencies η_M in different sections; (2) variable temperature

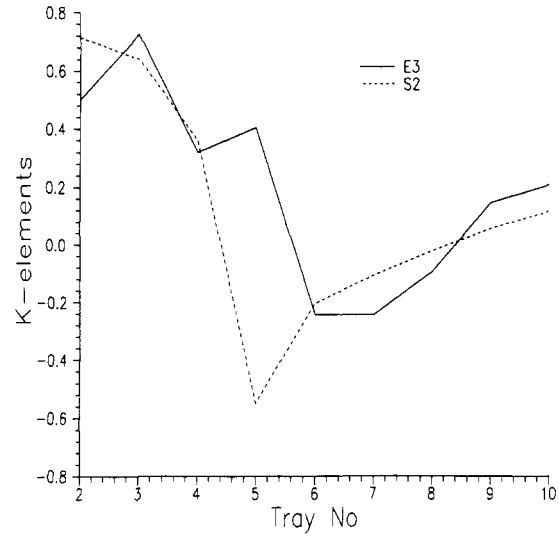

Figure 12. Elements in matrix **K** for x_B.

noise instead of constant noise in weight W_3 for S2, i.e., base the weight on Figure 5; and (3) constant feed temperature rather than assuming incorrectly that the feed is saturated liquid. For our experimental column the first proposal would probably have minor importance since the difference in performance between S1 and S2 is very small. The second proposal might have improved the estimate by giving a weight function W_3 that is more similar to the one used by E3, which would give the feed tray less weight. The last proposal would probably have the largest affect on the estimator. In the experimental column the feed temperature controller was set to a fixed value of 91 °C. This will not give a constant liquid fraction in the feed, as was assumed in the simulation runs.

The reason why we care about the simulation-based estimator is of course that experimental calibration runs may be difficult and time consuming to perform on industrial columns. In particular, it is difficult to ensure that all the "directions" in the space of independent variables (y_D, x_B, disturbances) are sufficiently exited. One may therefore have to rely also on simulations.

The problem is then to adapt the simulated estimator to the real column. Experimental data give a good representation of the true system, but it may be difficult to obtain reliable data which span the desired range of operation. On the other hand, simulations may not represent

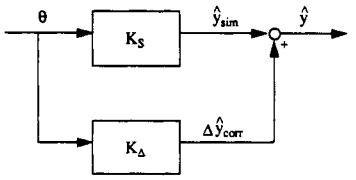

Figure 13. Block diagram for a combined estimator based on simulations ($\hat{y}_{sim}$) and corrected (Δy) using experimental data.

the true system as accurately, but it is easy to use the model to generate changes which are difficult to do experimentally. Also, there may be effects or disturbances on the real system which are not represented by the simulation model. This discussion leads to the conclusion that the optimal estimator should combine both simulated and experimental data. In some sense, this is already done since the simulation model is obtained by adjusting the tray efficiency to match the experimental data. However, the results in this paper show that this is not sufficient; that is, the experimental data contain additional information. One possible approach is shown in Figure 13.

$$\hat{y} = \hat{y}_{sim} + \Delta\hat{y}_{corr} = \mathbf{K}_S\theta + \mathbf{K}_\Delta\theta \qquad (13)$$

The overall estimator is $\mathbf{K} = \mathbf{K}_S + \mathbf{K}_\Delta$.

The basic idea is to use the simulation-based estimator, $\mathbf{K}_S$, to capture effects ("directions") due to different feed compositions and product composition which may be difficult to excite in the real column. This estimate is then corrected by the experimental "correction estimator", $\mathbf{K}_\Delta$. The simulation-based estimator $\mathbf{K}_S$ is obtained first. This gives rise to the estimate $\hat{y}_{sim}$. The correction $\Delta\hat{y}_{corr}$ is found from the available experimental runs. The data matrices for the correction estimator corresponding to eq 2 become

$$\Delta\mathbf{Y} = \mathbf{Y} - \mathbf{Y}_{sim} = \Theta_{exp}\mathbf{K}_\Delta^T \qquad (14)$$

For directions which are not exited in the experiments, the correction is only a constant term (bias), as for estimators S1 and S2. On the other hand, in directions where the experimental data have adequate excitations $\mathbf{K}_\Delta$ should use the entire temperature profile. One important issue will be to ensure that the noise and uncertainty in the experimentally obtained data runs do not corrupt the estimate, by for example using a conservative number of factors in the correcting estimator. This off-line approach for obtaining $\mathbf{K} = \mathbf{K}_S + \mathbf{K}_\Delta$ may include an updating procedure for $\mathbf{K}_\Delta$ to handle changes in the distillation column. Instead, to update $\mathbf{K}$, a simple way of on-line correction of the estimator is to adjust the bias term, $\mathbf{k}_0$, in eq 1.

7. Conclusions

This paper addresses the implementation of a partial-least-squares estimator on a pilot-scale distillation column. An experimentally based estimator, with logarithmically transformed temperatures and compositions, gave excellent performance over a wide range of operating points. The need for updating the estimator was minimal.

Estimators based on only simulated data showed reasonable performance. However, when a change was made to different operating points, the steady-state bias had to be corrected. An important area of future work is to find estimators which efficiently combine data based on simulations and experiments.

Acknowledgment

Financial support from the Royal Norwegian Council of Scientific and Industrial Research (NTNF) is gratefully acknowledged. Most of the calculations have been performed with the UNSCRAMBLER software package provided by H. Martens.

Nomenclature

B = bottom-product flow rate
D = distillate flow rate
F = feed rate
$\mathbf{E}_k$ = residual data matrix of the temperatures after extracting k factors
E1–E3 = estimators based on *experimental* calibration runs
$\mathbf{K}$, $\mathbf{k}_0$ = estimator constants
L = reflux flow rate
L_θ = logarithmic temperatures based on reference temperatures
s_{ei} = residual standard deviation of temperature on tray i
S1, S2 = estimators based on *simulations*
V = boilup from reboiler
x_B = mole fraction of light component in bottom product
y_D = mole fraction of light component in distillate
$\mathbf{y}$ = output vector $(y_D, x_B)^T$
z_F = mole fraction of light component in feed

Greek Symbols

η_M = Murphree tray efficiency
θ = tray temperature
θ = tray temperature vector
Θ = data matrix of θ

Subscripts

c = term from calibration set
e = error term
i = tray number (ordered from the bottom)
0 = average (bias) term

Literature Cited

Boyd, D. M., Jr. Fractionation Column Control. *Chem. Eng. Prog.* **1975**, *71*, 55–60.

Bozenhardt, H. F. Modern control tricks solve distillation problems. *Hydrocarbon Process.* **1988**, *67* (6), 47–50.

Gay, L. Distillation et Rectification des Mélanges complexes. *Chim. Ind.* **1927**, *18*, 187–203.

Hellwig, L. R.; van Winkle, M. Vapor-Liquid Equilibria for Alcohol Binary Systems. *Ind. Eng. Chem.* **1953**, *45*, 624–629.

Höskuldsson, A. PLS Regression Methods. *J. Chemom.* **1988**, *2*, 211–228.

Joseph, B.; Brosilow, C. B. Inferential Control of Processes. Part I. Steady State Analysis and Design. *AIChE J.* **1978**, *24*, 485–492.

Joseph, B.; Brosilow, C. B.; Howell, J. C.; Kerr, W. R. D. Multi-temps give better control. *Hydrocarbon Process.* **1976**, *3*, 127–131.

Kalman, R. E.; Bucy, R. S. New results in Linear Filtering and Prediction Theory, ASME. *J. Basic Eng.* **1961**, *83*, 95–108.

Kister, H. Z. *Distillation Operation*; McGraw-Hill: New York, 1990; p 545.

Luyben, W. L. Feedback Control of Distillation Columns by Double Differential Temperature Control. *Ind. Eng. Chem. Res.* **1969**, *8*, 739–744.

Luyben, W. L. Control of Distillation Columns with Sharp Temperature Profiles. *AIChE J.* **1971**, *17*, 713–718.

Luyben, W. L. Simple Method for Tuning SISO Controllers in Multivariable Systems. *Ind. Eng. Chem. Res.* **1986**, *25*, 654–660.

Marquardt, W. Concentration profile estimation and control in binary distillation. *Proceedings of the IFAC Workshop, Model Based Process Control*, Atlanta, GA, 13–14 June 1988; McAvoy, T. J., et al., Eds.; International Federation of Automatic Control, Pergamon Press: Oxford, U.K., 1989.

Martens, H.; Næs, T. *Multivariate Calibration*; Wiley: New York, 1989.

Mejdell, T. Estimators for Product Compositions in Distillation Columns. Ph.D. Thesis, University of Trondheim, NTH, 1990.

Mejdell, T.; Skogestad, S. Output estimation for ill-conditioned plants using multiple secondary measurements: High-purity distillation. Submitted to *Automatica* **1991a** (also presented at the 1990 AIChE meeting, Chicago, Paper 23g).

Mejdell, T.; Skogestad, S. Estimation of Distillation Compositions from Multiple Temperature Measurements Using Partial-Least-

Squares Regression. *Ind. Eng. Chem. Res.* **1991b**, preceding paper in this issue.
Rademaker, O.; Rijnsdorp, J. E.; Maarleveld, A. *Dynamics and Control of Continuous Distillation Units*; Elsevier: Amsterdam, 1975.
Skogestad, S.; Lundström, P. Mu-optimal LV-control of Distillation Columns. *Comput. Chem. Eng.* **1990**, *14* (4/5), 401-413.
Weber, R.; Brosilow, C. B. The Use of Secondary Measurements to Improve Control. *AIChE J.* **1972**, *18*, 614-623.
Whitehead, D. B.; Parnis, M. Computer control improves ethylene plant operation. *Hydrocarbon Process.* **1987**, 105-108.
Yu, C. C.; Luyben, W. L. Use of Multiple Temperatures for the Control of Multicomponent Distillation Columns. *Ind. Eng. Chem. Res.* **1984**, *23*, 590-597.

Received for review March 19, 1991
Accepted July 23, 1991

Direct and Indirect Model Based Control Using Artificial Neural Networks

Dimitris C. Psichogios and Lyle H. Ungar*
Department of Chemical Engineering, University of Pennsylvania, Philadelphia, Pennsylvania 19104-6393

The use of artificial neural networks in model based control, both as process models and as controllers, is investigated: two nonlinear model based control strategies, internal model control (IMC) and multistep predictive control (MPC), are applied to the control of a nonlinear SISO exothermic CSTR. Direct inverse control in the IMC framework was found to require appropriate use of feedback for adequate performance. An IMC-type neural network controller in which the process model was replaced by a nonlinear neural network and inverted on-line to calculate the control action gave very good performance, even when only partial state data were available. An MPC-type neural controller using the same neural network model and extended to include feedback also gave excellent performance. Performance was significantly better for both control techniques when a nonlinear network was used as a process model than when a linear ARMAX model was used. These results indicate that neural networks can learn sufficiently accurate models and give good nonlinear control when model equations are not known or only partial state information is available.

1. Introduction

Multilayered feedforward neural networks represent a special form of connectionist model that performs a mapping from an input space to an output space. They consist of massively interconnected simple processing elements (neurons or nodes) arranged in a layered structure; the strength of each connection is characterized by its assigned weight. The input neurons are connected to the output neurons through layers of hidden nodes. The processing of information in each neuron is performed through its activation function: when the hidden units have a nonlinear activation function the mapping is nonlinear. Such networks can approximate any nonlinear continuous function arbitrarily accurately. Training of the network—essentially adjustment of the weights—is performed by an appropriate algorithm, such as error backpropagation (Werbos, 1974; Rumelhart et al., 1986), and through repeated presentation of a set of input-output patterns. Neural networks can learn associations—or classification—of events, in applications such as fault diagnosis (Ungar et al., 1990), or they can be used, as we will do in this paper, to extract the underlying quantitative relationships governing the behavior of physical systems.

Neural nets have been successfully used to identify dynamical systems which exhibit complicated behavior, such as deterministic chaos (Lapedes and Farber, 1987; Ydstie, 1990; Levin, 1990), chaotic chemical systems (Admoaitis et al., 1990), chemical reactions (Bhat and McAvoy, 1990), and other nonlinear SISO and MIMO systems (Narendra and Parthasarathy, 1990). More recently neural nets are starting to be used for control problems such as manipulating robot arms (Jordan, 1988, 1990; Guez et al., 1988; Miller, 1989) and controlling chemical processes (Donat et al., 1990; Ydstie, 1990; Hernandez and Arkun, 1990), in a variety of controller architectures.

One of the most studied control strategies is model based control (MBC), where a process model is explicitly used to predict future process behavior, the same process model is also implicitly used (essentially inverted) to calculate the control action in such a way as to satisfy the controller's design specifications. In this way information about the dynamical system is used to give performance superior to that of traditional control techniques, such as PID controllers. Control theory has been extensively developed for linear systems, yet linear control strategies have been shown to perform poorly when applied to certain nonlinear systems (Economou et al. 1986; Parrish and Brosilow, 1988). Furthermore, we are far from being able to optimally design controllers that can handle time-varying and uncertain dynamical systems; adaptive linear control methods can result in suboptimal performance (Morningred et al., 1990). It is not surprising, therefore, that much of the current research effort is focused on developing robust nonlinear control techniques, which give good performance in spite of unmodeled or time-varying dynamics. In this context, artificial neural networks promise to provide a flexible basis for adaptive nonlinear controllers.

In process control applications neural networks can be incorporated in the controllers in either direct or indirect control methods. In the direct method, a neural network is trained with observed input-output data from the system to represent its inverse dynamics. In other words, given the current state of the dynamic system and the target state (e.g., setpoint) for the next sampling instant, the network is trained to produce the control action that drives the system to this target state. The resulting inverse model neural network can then be used as a controller, typically in a feedforward fashion. In the indirect method

* Author to whom correspondence should be addressed.

0888-5885/91/2630-2564$02.50/0